

Technical report 11-029

# **Variable speed limits for green mobility\***

S.K. Zegeye, B. De Schutter, J. Hellendoorn, and E.A. Breunese

*If you want to cite this report, please use the following reference instead:*

S.K. Zegeye, B. De Schutter, J. Hellendoorn, and E.A. Breunese, “Variable speed limits for green mobility,” *Proceedings of the 14th International IEEE Conference on Intelligent Transportation Systems (ITSC 2011)*, Washington, DC, pp. 2174–2179, Oct. 2011.

Delft Center for Systems and Control  
Delft University of Technology  
Mekelweg 2, 2628 CD Delft  
The Netherlands  
phone: +31-15-278.24.73 (secretary)  
URL: <https://www.dcsc.tudelft.nl>

---

\*This report can also be downloaded via [https://pub.deschutter.info/abs/11\\_029.html](https://pub.deschutter.info/abs/11_029.html)

# Variable Speed Limits for Green Mobility

S. K. Zegeye, B. De Schutter, J. Hellendoorn, and E. A. Breunesse

**Abstract**—Due to increasing environmental concerns the focus of traffic management and control is shifting towards optimizing the traffic control measures to also reduce traffic emissions and fuel consumption. In this context we propose a model-based predictive traffic control approach for the balanced reduction of travel times, emissions, and fuel consumption for freeway networks, where not only the local emissions are taken into account but also the dispersion of the emissions to various target zones near the freeways. The core of the approach is a new efficient model for describing the area-wide dispersion of the emissions that is much faster than the models we have proposed in earlier papers. We present a detailed description of the new so-called expanding grid-based model and we embed it in a model-based predictive traffic control approach using variable speed limits.

## I. INTRODUCTION

This paper proposes a traffic control approach for reducing the emissions both locally on the freeway as well as their dispersion to one or more so-called target zones. In addition, the approach we propose can also be used to reduce fuel consumption, and as such contributes to a more sustainable and greener mobility through active traffic management and control.

Reducing the amount of emitted gases of the traffic flow will improve the overall emission levels. However, since dispersion of the emissions is also dependent on the wind, temperature, rainfall, and terrain of the neighborhood of the freeway, the dispersion of the emissions can be distributed unevenly. This means that certain areas can face higher emission levels. E.g., public areas could face higher emission levels despite the reduced total emission levels at the network level, because other factors such as wind and temperature can locally affect the concentration of the emitted gases. Therefore, it is not smart to control the emissions for the whole freeway at all times, but it is better to focus on the parts of the freeway that affect the target zones and on the time windows in which the corresponding emissions originate. This could be done by predicting the evolution of the emissions and their dispersion towards the target zones. So a predictive control approach is required.

It is well-known that in general improved traffic flows can have severe consequences on the emission levels [1]. On the other hand, focusing exclusively on reduction of emissions (or fuel consumption) will in general have a negative effect on other performance measures, such as

travel times or throughput [2]. Therefore, a control approach is required that can provide a balanced trade-off between various performance objectives. In this context and also due to the need for taking into account the predicted future effects of current control actions, we advocate the use of model-based predictive control (MPC) [3]. Although MPC has originated in the process industry, it has been extended to several other fields, including traffic management [4]–[9].

Despite the fact that conventional MPC has proven to be a potentially very effective traffic control strategy in [4]–[9], it is not tractable in practice due to its heavy computational demands. Therefore, we adopt an alternative approach in this paper, called parametrized MPC. Parametrized MPC starts from parametrized (feedback) control laws and optimizes the parameters of these control laws instead of the control input sequences. Since the number of parameters to be optimized is in general much smaller than the number of control inputs, parametrized MPC requires much lower computation times than conventional MPC.

An important element in MPC are the prediction models. As MPC is an on-line optimization-based control strategy, it requires running the prediction models repeatedly at each control step. Hence, these models have to provide a balanced trade-off between computation speed and accuracy. For modeling of traffic flows and of emissions several efficient models have been developed [10]–[12]. However, for describing the evolution of emissions in the more remote neighborhood of the freeways (i.e., the dispersion of emissions) models that well fit into the MPC framework are still being developed.

In [13], [14] we have developed a basic dispersion model based on the use of point sources for use in an MPC framework. This model was later on extended [15] to include variable wind speed and variable wind direction, and to allow spatially more uniformly distributed emission sources. However, these models do not deal properly with low wind speed situations, and they are computationally intensive. In this paper we therefore propose a new dispersion model that addresses these shortcomings and that is therefore excellently suited for use in MPC approach for traffic control. In combination with parametrized MPC this yields a control approach that is very fast and that provides almost the same performance as conventional MPC.

## II. TRAFFIC FLOW AND EMISSION MODELS

Since the MPC approach we adopt requires models, we first provide a concise recapitulation of the traffic flow and emission models we consider for this paper, viz. the METANET traffic flow model and the VT-macro emissions

S. K. Zegeye, B. De Schutter, and J. Hellendoorn are with the Delft Center for Systems and Control, Delft University of Technology, Delft, The Netherlands. E. A. Breunesse is with Shell Nederland B.V. The Hague, The Netherlands {s.k.zegeye, b.deschutter, j.hellendoorn}@tudelft.nl, ewald.breunesse@shell.com

and fuel consumption model. Note, however, that the proposed approach is generic and that other prediction models can also be used, provided they are sufficiently fast and provided that they capture the essential characteristics of the traffic flow and of the emissions.

#### A. METANET

The METANET model [10], [11] is a second-order macroscopic traffic flow model that describes the traffic behavior using aggregate variables, such as average traffic flow ( $q$ ), density ( $\rho$ ), and space-mean speed ( $v$ ). The METANET model represents a traffic network model as a graph with nodes (corresponding to mainstream origins, on-ramps, off-ramps, merges, splits, lane drops) and links (corresponding to homogeneous stretches of freeway) connecting the nodes. Links are further divided into segments of length 500–1000 m. The traffic dynamics in segment  $i$  of link  $m$  are<sup>1</sup>

$$\begin{aligned} q_{m,i}(k) &= \lambda_m \rho_{m,i}(k) v_{m,i}(k) & (1) \\ \rho_{m,i}(k+1) &= \rho_{m,i}(k) + \frac{T}{L_m \lambda_m} [q_{m,i-1}(k) - q_{m,i}(k)] & (2) \\ v_{m,i}(k+1) &= v_{m,i}(k) + \frac{T}{\tau} [V[\rho_{m,i}(k)] - v_{m,i}(k)] \\ &+ \frac{T v_{m,i}(k) [v_{m,i-1}(k) - v_{m,i}(k)]}{L_m} \\ &- \frac{T \eta [\rho_{m,i+1}(k) - \rho_{m,i}(k)]}{\tau L_m (\rho_{m,i}(k) + \kappa)} & (3) \end{aligned}$$

$$V[\rho_{m,i}(k)] = \min \left\{ (\alpha_m + 1) u_{m,i}(k), v_{\text{free},m} \exp \left[ -\frac{1}{a_m} \left( \frac{\rho_{m,i}(k)}{\rho_{\text{cr},m}} \right)^{a_m} \right] \right\} \quad (4)$$

with  $q_{m,i}(k)$ ,  $\rho_{m,i}(k)$ , and  $v_{m,i}(k)$  respectively the flow, density, space-mean speed in segment  $i$  of link  $m$  at simulation step  $k$ ,  $u_{m,i}(k)$  the variable speed limit in segment  $i$  of link  $m$  at simulation step  $k$ ,  $v_{\text{free},m}$  the free-flow speed,  $\alpha_m$  the compliance factor of the drivers,  $L_m$  the length of the segments of link  $m$ ,  $\lambda_m$  the number of lanes of link  $m$ , and  $T$  the simulation time step size. Furthermore,  $\rho_{\text{cr},m}$  is the critical density, and  $\tau$ ,  $\eta$ ,  $\kappa$ ,  $a_m$  are model parameters.

For origins a queue model is used. The evolution of the queue length  $w_o$  at the origin  $o$  is modeled as

$$w_o(k+1) = w_o(k) + T(d_o(k) - q_o(k))$$

where  $d_o$  and  $q_o$  denote respectively the demand and outflow of origin  $o$ . The outflow  $q_o$  is given by<sup>2</sup>

$$q_o(k) = \min \left[ d_o(k) + \frac{w_o(k)}{T}, C_o \left( \frac{\rho_{\text{jam},m} - \rho_{m,1}(k)}{\rho_{\text{jam},m} - \rho_{\text{cr},m}} \right) \right],$$

with  $\rho_{\text{jam},m}$  the maximum density of link  $m$ , and  $C_o$  the capacity of the origin  $o$ . Refinements and extensions of the above model are discussed in [5], [10], [11].

<sup>1</sup>The desired speed  $V[\rho_{m,i}(k)]$  in (4) is taken from [5].

<sup>2</sup>For a metered on-ramp, an extra term  $r_o(k)C_o$  (with  $r_o(k) \in [0, 1]$  the ramp metering rate) is added as argument of the min operator.

#### B. VT-macro

The VT-macro model [12] is a macroscopic emission model and fuel consumption that is based on the microscopic model VT-micro [16] and that is in particular developed for the METANET traffic flow model. In the VT-macro model a distinction is made between the temporal and spatial-temporal accelerations and number of vehicles subject to it. The temporal acceleration and the corresponding number of vehicles for (or better, staying in) segment  $i$  of link  $m$  at time step  $k$  are given by

$$\begin{aligned} a_{m,i}(k) &= \frac{v_{m,i}(k) - v_{m,i}(k-1)}{T} \\ n_{m,i}(k) &= L_m \lambda_m \rho_{m,i}(k) - T \lambda_m v_{m,i-1}(k-1) \rho_{m,i-1}(k-1). \end{aligned}$$

The spatial-temporal acceleration is different for different freeway geometries. For brevity, we only consider spatial-temporal accelerations of links here. The spatial-temporal acceleration and the number of vehicles going from segment  $i$  to segment  $i+1$  of a link  $m$  at time step  $k$  are given by

$$\begin{aligned} a_{m,i,i+1}(k) &= \frac{v_{m,i+1}(k) - v_{m,i}(k-1)}{T} \\ n_{m,i,i+1}(k) &= T q_{m,i}(k-1). \end{aligned}$$

Similar equations can be derived for on-ramps, off-ramp, and junctions (see [12] for details).

Using the temporal and spatial-temporal components of the space-mean speed, acceleration, and number of vehicles, the VT-macro model is expressed as

$$\begin{aligned} J_{y,m,i}(k) &= n_{m,i}(k) \exp \left( S^T(v_{m,i}(k-1)) P_y S(a_{m,i}(k)) \right) \\ &+ n_{m,i,i+1}(k) \exp \left( S^T(v_{m,i}(k)) P_y S(a_{m,i,i+1}(k)) \right) \end{aligned}$$

where  $J_{y,m,i}(k)$  [kg/s] is the estimate or prediction of the emission (for  $y \in \{\text{CO}, \text{NO}_x, \text{HC}\}$ ) or fuel consumption (for  $y = \text{FC}$ ) variable for segment  $i$  of link  $m$  during the time period  $[kT, (k+1)T]$ , and where the  $S$  operator yields a vector defined as  $S(x) = [1 \ x \ x^2 \ x^3]^T$  for a scalar input argument  $x$ . The values of the parameter matrices  $P_y$  can be found in [16]. Moreover, from the fuel consumption  $J_{\text{FC},m,i}(k)$  one can compute the  $\text{CO}_2$  emissions value  $J_{\text{CO}_2,m,i}(k)$  [12], [17].

### III. EXPANDING GRID-BASED DISPERSION MODEL

Dispersion of vehicular emissions is affected by several factors, including the speed of the vehicles, the weather conditions, and the geometry and topology of the freeway area. Apart from the topology, in the vicinity of the freeway the speeds of the vehicles mainly influence the dispersion of the emissions [18], while in the region far from the road, the dispersion of the emissions is primarily dependent on the wind and the temperature of the atmosphere [18].

Now we propose a new dispersion model that addresses several of the shortcomings of the point-source model and its extension we introduced in [13]–[15]. In particular, the new model addresses the computational complexity issues of the basic point-source model, and it also incorporates the effect of varying wind speed, wind direction, and temperature on the dispersion of the emissions. Note that we focus on

the 2D effects of the dispersion as we are interested in the emission levels at ground level; the dispersion into the vertical direction is modeled via an “evaporation” factor  $\gamma$ .

### A. Main idea

In the point-source model [13], [14] and its extension [15] the dispersion of the emissions is modeled under the assumption that the emission wavefronts are straight lines and diverge within so-called dispersion cones, with a dispersion angle that is dependent on the speed of the wind. For no-wind conditions, the dispersion angle is modeled correctly, but the dispersion itself is not. Indeed, if the wind speed is zero, then the emissions do not move in those models, which means that then there is no dispersion of the emissions over the horizontal 2D plane, which does not correspond to reality at all. This problem could be solved by adding a term that is dependent on the temperature and the inherent dispersion factors of the emissions. But, since the point-source dispersion model and its extension are based on the assumption that the emission wavefronts move as straight lines, which is valid under higher wind speeds, the added term will result in emissions moving in one direction only without dispersing sideways. Hence, another modeling approach is required.

If one would consider the dispersion wavefront to be a curve instead of a straight line, under no-wind conditions this curve would be a circle with a radius that increases according to the expansion factor of the emissions. It is this analysis that led to the development of the expanding grid-based dispersion model. For this model, under no-wind conditions and with no other external disturbances emissions will correctly expand in all directions.

### B. Expanding grid-based model

First, we grid the region around the freeway into squares of equal dimensions. The center of each cell is considered as a representative of the emissions in that cell. Although the cells in this expanding grid-based dispersion modeling approach are squares, and the expansion using curved dispersion wavefronts would result in distorted squares, we will represent these distorted squares by regular squares in order to get a fast and efficient approximate dispersion model.

Let the wind speed at time step  $k$  be denoted by  $V_w(k)$  and let the angle of the wind w.r.t the  $x$ -axis be denoted by  $\phi(k)$  (with positive angles in the clockwise direction). Moreover, we denote the expansion factor of the emissions of the grid at time step  $k$  cells by  $\varpi(k)$  per unit time in each direction. Hence, when the wind speed is zero, at time step  $k$  the emissions in the cell  $C_{i_c, j_c}$  expand as illustrated by the light-blue shaded region in Fig. 1(a), resulting in an expanded square with equal sides of length  $(1 + T\varpi(k))L$ , where  $L$  is the length of the sides of the grid cells.

When the wind speed is non-zero, the expanded emission square of cell  $C_{i_c, j_c}$  is displaced in the wind direction as depicted in Fig. 1(b). We use the center point of the expanded emission square to represent the displacement of the square. The corner points of the expanded emission square can be

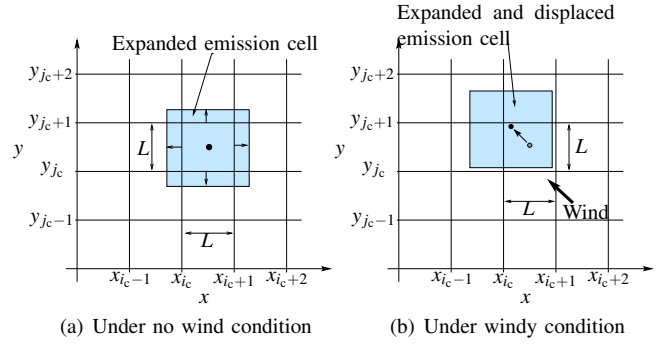


Fig. 1. Expansion of emissions from a cell under windy and no wind conditions.

determined from the coordinates of the displaced center point and the expansion factor.

Let us now determine the emission level in cell  $C_{i_c, j_c}$ . It is important to note that for the expanding grid-based model it is possible to explicitly describe the equation of the intersections between the expanded emission squares and the original grid cells with simple equations that are moreover valid for all cells. This is a major difference with the point-source model and its extension, which use much more complex expression that also depend on the spatial coordinates of the emission sources.

So, let us suppose the level of the emission  $y$  at time step  $k$  in cell  $C_{i_c, j_c}$  is  $J_{y, i_c, j_c}(k)$ , then at the end of the time period  $[kT, (k+1)T)$  the emission level in the cell becomes

$$J_{y, i_c, j_c}(k+1) = J_{\text{src}, y, i_c, j_c}(k) + (1 - \gamma(k)) \sum_{(u_c, v_c) \in \mathcal{N}(i_c, j_c)} \frac{\alpha_{(i_c, j_c)}^{(u_c, v_c)}(k)}{(1 + T\varpi(k))^2 L^2} J_{y, u_c, v_c}(k) \quad (5)$$

where  $J_{\text{src}, y, i_c, j_c}(k)$  is the emissions generated by the traffic (and other sources) within cell  $C_{i_c, j_c}$  in the period  $[kT, (k+1)T)$ ,  $\alpha_{(i_c, j_c)}^{(u_c, v_c)}(k)$  is the area of the part of the expanded emission square of neighboring cell  $C_{u_c, v_c}$  that intersects the cell  $C_{i_c, j_c}$  at time step  $k$ ,  $\mathcal{N}(i_c, j_c)$  is the set of neighboring cells of cell  $C_{i_c, j_c}$  and cell  $C_{i_c, j_c}$  itself, and  $\gamma(k)$  is the vertical dispersion factor. Using simple geometrical arguments it can be shown that the expressions for  $\alpha_{(i_c, j_c)}^{(u_c, v_c)}(k)$  are<sup>3</sup>

$$\begin{aligned} \alpha_{(i_c, j_c)}^{(i_c-1, j_c-1)}(k) &= \max\{0, b_2(k)\} \cdot \max\{0, b_1(k)\} \\ \alpha_{(i_c, j_c)}^{(i_c, j_c-1)}(k) &= (L - \max\{0, -b_0(k), -b_1(k)\}) \cdot \max\{0, b_2(k)\} \\ \alpha_{(i_c, j_c)}^{(i_c+1, j_c-1)}(k) &= \max\{0, b_0(k)\} \cdot \max\{0, b_2(k)\} \\ \alpha_{(i_c, j_c)}^{(i_c-1, j_c)}(k) &= \max\{0, b_1(k)\} \cdot (L - \max\{0, -b_2(k), -b_3(k)\}) \\ \alpha_{(i_c, j_c)}^{(i_c, j_c)}(k) &= (L - \max\{0, -b_0(k), -b_1(k)\}) \\ &\quad \cdot (L - \max\{0, -b_2(k), -b_3(k)\}) \end{aligned}$$

<sup>3</sup>We assume here that the expanded emission squares only cover the immediate neighbors of cell  $C_{i_c, j_c}$  and/or cell  $C_{i_c, j_c}$  itself, but no other cells. In case other cells are also covered (this may happen if the wind speed  $V_w(k)$  or the expansion factor  $\varpi(k)$  are large), similar formulas for an extended neighborhood set  $\mathcal{N}(i_c, j_c)$  can be derived.

$$\alpha_{(i_c, j_c)}^{(i_c+1, j_c)}(k) = \max\{0, b_0(k)\} \cdot (L - \max\{0, -b_2(k), -b_3(k)\})$$

$$\alpha_{(i_c, j_c)}^{(i_c-1, j_c+1)}(k) = \max\{0, b_3(k)\} \cdot \max\{0, b_1(k)\}$$

$$\alpha_{(i_c, j_c)}^{(i_c, j_c+1)}(k) = (L - \max\{0, -b_0(k), -b_1(k)\}) \cdot \max\{0, b_3(k)\}$$

$$\alpha_{(i_c, j_c)}^{(i_c+1, j_c+1)}(k) = \max\{0, b_0(k)\} \cdot \max\{0, b_3(k)\}$$

where

$$b_0(k) = \frac{LT\varpi(k)}{2} + TV_w(k) \cos(\varphi(k))$$

$$b_1(k) = \frac{LT\varpi(k)}{2} - TV_w(k) \cos(\varphi(k))$$

$$b_2(k) = \frac{T\varpi(k)}{2} + TV_w(k) \sin(\varphi(k))$$

$$b_3(k) = \frac{LT\varpi(k)}{2} - TV_w(k) \sin(\varphi(k)).$$

Note that the computation of the above intersections gives the same result for all the cells in the grid. This means that the computation has to be done only for one cell at each simulation time step  $k$ .

The total emission level at the target zone  $Z_t$  is therefore computed by summing up the fraction of the emissions contributed by each cell that intersects the target zone  $Z_t$ . Hence, at time step  $k$  it is given by

$$D_{y,t}(k) = \sum_{(i_c, j_c) \in \mathcal{I}_{\text{int},t}} \frac{\text{area}(C_{\text{target},t} \cap C_{i_c, j_c})}{A_{i_c, j_c}} J_{y, i_c, j_c}(k)$$

where  $C_{\text{target},t}$  is the cell (or more general, polytope) description of the target zone  $Z_t$  and  $\mathcal{I}_{\text{int},t}$  is the set of all cells in the grid that have common area with the target zone  $Z_t$ .

#### IV. PARAMETRIZED MPC FOR GREEN MOBILITY

##### A. General concept of MPC

Conventional MPC [3] uses a model of a system to predict the evolution of the state of the system for a sequence of control inputs using the current state of the system as the initial condition. Based on the predicted states of the system, the controller determines the value of a given cost function and optimizes the sequence of control inputs over the prediction horizon to minimize the cost function. Next, only the first control input of the optimal sequence is applied to the system until the next control time step, after which the controller repeats the above process all over again using a moving horizon principle.

##### B. MPC performance measure

We consider a multi-objective performance criterion that accommodates the total time spent (TTS), total emission (TE), and the total maximum dispersion level (TMDL) of emissions, as well as variations in time and space of the control signal. Let  $T_c$  be the control step size<sup>4</sup>. At control

<sup>4</sup>For the sake of simplicity we assume that the control step size  $T_c$  and the simulation step size  $T$  are related by  $T_c = MT$ , for some positive integer  $M$ . Therefore, at time instant  $t = k_c T_c = kT$  the control step counter  $k_c$  is an integer divisor of the simulation step counter  $k$ . They are then related by  $k(k_c) = Mk_c$ .

step  $k_c$ , the multi-objective function is defined as a weighted sum of the constituents and it is given by

$$J(k_c) = \zeta_1 \frac{\text{TTS}(k_c)}{\text{TTS}_n} + \zeta_2 \frac{\text{TE}(k_c)}{\text{TE}_n} + \zeta_3 \frac{\text{TMDL}(k_c)}{\text{TMDL}_n} + \zeta_4 \Delta(k_c) \quad (6)$$

where

$$\begin{aligned} \text{TTS}(k_c) &= T \sum_{k=Mk_c}^{M(k_c+N_p)-1} \left( \sum_{(m,i) \in \mathcal{I}_{\text{all}}} \lambda_m L_m \rho_{m,i}(k) + \sum_{o \in \mathcal{O}_{\text{all}}} w_o(k) \right), \\ \text{TE}(k_c) &= \sum_{y \in \mathcal{Y}} \mu_y \frac{\text{TE}_y(k_c)}{\text{TE}_{n,y}}, \quad \text{TMDL}(k_c) = \sum_{y \in \mathcal{Y}} \mu_y \frac{\text{TD}_y(k_c)}{\text{TD}_{n,y}}, \\ \Delta(k_c) &= \sum_{k=Mk_c}^{M(k_c+N_p)-1} \left\{ \sum_{s \in \mathcal{S}_{\text{all}}} \alpha_s (u_s(k) - u_s(k-1))^2 \right. \\ &\quad + \sum_{(s_1, s_2) \in \mathcal{P}_{\text{all}}} \alpha_{cs} (u_{s_1}(k) - u_{s_2}(k))^2 \\ &\quad \left. + \sum_{r \in \mathcal{R}_{\text{all}}} \alpha_r (u_r(k) - u_r(k-1))^2 \right\}, \end{aligned}$$

$$\text{with TE}_y(k_c) = \sum_{k=Mk_c}^{M(k_c+N_p)-1} \sum_{(m,i) \in \mathcal{I}_{\text{all}}} J_{y,m,i}(k),$$

$$\text{TD}_y(k_c) = \sum_{t \in \mathcal{T}_{\text{all}}} \max_{k=Mk_c, \dots, M(k_c+N_p)-1} D_{y,t}(k)$$

where  $N_p$  is the prediction horizon,  $\zeta_i \geq 0$  for  $i = 1, 2, 3, 4$ , and  $\mu_y \geq 0$  are the weights,  $\mathcal{Y} = \{\text{CO}, \text{NO}_x, \text{HC}, \text{FC}, \text{CO}_2\}$ ,  $\mathcal{O}_{\text{all}}$  is the set of all origins in the traffic network,  $\mathcal{I}_{\text{all}}$  is the set of all segments of links in the traffic network,  $\mathcal{S}_{\text{all}}$  is the set of all speed limits,  $\mathcal{P}_{\text{all}}$  is the set of all consecutive speed limits,  $\mathcal{R}_{\text{all}}$  is the set of all target zones, and  $\alpha_r = (\#\mathcal{R}_{\text{all}} N_p)^{-1}$ ,  $\alpha_s = (\#\mathcal{S}_{\text{all}} N_p v_{\text{step}}^2)^{-1}$ , and  $\alpha_{cs} = (\#\mathcal{P}_{\text{all}} N_p v_{\text{step}}^2)^{-1}$  are normalization factors with  $v_{\text{step}}$  denoting a nominal maximum change of speed limit between different segments and time steps, and  $\#(\cdot)$  denoting the set cardinality. Moreover, the subscript ‘n’ denotes nominal values of TTS, TE,  $\text{TE}_y$ , TMDL, and  $\text{TD}_y$ .

##### C. Parametrized MPC for traffic control

Many traffic control researchers have shown that MPC can improve the performance of road networks [4]–[9]. Nonetheless, as a consequence of its high computation demands, conventional MPC using advanced traffic models has not yet found its way to practice<sup>5</sup>. One way to reduce the computation time of the MPC controller is to parametrize the control inputs using a control law with a limited number of parameters [21]–[24]. In general, this will reduce the computation time significantly.

We have proposed such an approach in the context of MPC for traffic control in [14]. To illustrate this idea, we now

<sup>5</sup>One could consider strategies like SCOOT [19] and UTOPIA/SPOT [20] to be MPC, but they only use very simple models.

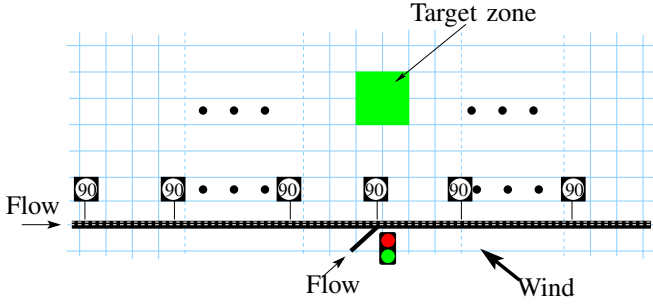


Fig. 2. A 12 km three lane freeway stretch considered for this study. Each cell in the grid is 200 m by 200 m.

present this approach for the case of variable speed limits<sup>6</sup>. Note however that the parametrization is just an illustration of the control approach, but that the control approach is generic and that it can also be used with other control laws and other control measures (such as, e.g., ramp metering). The control law for the variable speed limits can be defined as follows [14]

$$u_{sl,m,i}(k_c + j + 1) = \theta_{0,m} v_{free,m} + \theta_{1,m} \frac{v_{m,i+1}(k_c) - v_{m,i}(k_c)}{v_{m,i+1}(k_c) + \kappa_v} + \theta_{2,m} \frac{\rho_{m,i+1}(k_c) - \rho_{m,i}(k_c)}{\rho_{m,i+1}(k_c) + \kappa_p}$$

for  $j = 0, 1, \dots, N_p - 1$ , where  $\kappa_v$  and  $\kappa_p$  are fixed parameters introduced to prevent division by 0.

The proposed parametrization has only 3 parameters per link  $m$  (one could also vary  $\theta_{j,m}$  over the prediction horizon and/or consider the same parameters for all links) to be optimized in the parametrized MPC control strategy. This means that the speed limit controller can reduce the computation time if it is used with a freeway that has more than three independent variable speed limits or more than three prediction horizon steps (since there are at least  $3 \times N_p$  speed limit variables over the prediction horizon)<sup>7</sup>.

#### D. Overall MPC problem

If we consider the minimization of the control objective  $J(k_c)$  over the set of all parameter values  $\theta$  subject to the model equations, the parametrized control laws, and the operational constraints, we get in general a nonlinear non-convex optimization problem. This problem can be solved using global or multi-start local optimization methods [25] such as multi-start sequential quadratic programming, pattern search, genetic algorithms, or simulated annealing.

### V. CASE STUDY

We consider a 12 km freeway stretch that has three lanes. The freeway is divided into 12 segments with each of length

<sup>6</sup>For the sake of compactness, we will mainly focus on variable speed limit control in the exposition. However, the proposed approach can straightforwardly be extended to include other control measures too, such as ramp metering, mainstream metering, etc. E.g., in the case study of Section V we consider both variable speed limits and ramp metering.

<sup>7</sup>Using a similar reasoning we can define the parametrization of the ramp metering controller to be  $u_{r,m,i}(k_c + j + 1) = u_{r,m,i}(k_c + j) + \theta_{3,m} (\rho_{cr,m} - \rho_{m,i}(k_c + j)) / \rho_{cr,m}$  for  $j = 0, 1, \dots, N_p - 1$  [14]

TABLE I  
PERFORMANCE OF PARAMETRIZED MPC FOR THE DIFFERENT CONTROL OBJECTIVES. THE PERCENTAGE VALUES INDICATE THE RELATIVE CHANGE WITH RESPECT TO THE UNCONTROLLED SCENARIO.

Objective	Performance measure		
	TTS [veh-h]	TE [kg]	TMDL [ $\mu$ g]
Uncontrolled	1362.1	127.5	9896.3
TTS	875.8 (-35.7%)	141.5 (+11.0%)	12896.0 (+30.3%)
TE	1611.4 (+18.3%)	66.2 (-48.1%)	4819.6 (-51.3%)
TMDL	1604.6 (+17.8%)	66.4 (-47.9%)	4831.5 (-51.2%)
10TTS+TE+TMDL	1525.6 (+12.0%)	70.6 (-44.6%)	5517.4 (-44.3%)

1 km and equipped with a variable speed limit. The 6th segment of the freeway has a metered on-ramp (see Fig. 2). Moreover, we consider a target zone that is 1 km away from the middle of the segment with the on-ramp (see Fig. 2). The target zone has an area of 400 m  $\times$  400 m. A time-varying traffic demand both at the mainstream origin and the on-ramp origin is considered. The neighborhood of the freeway is considered to be flat with no obstructions and is subject to varying wind speed and wind direction. For this case study, we consider the wind speed  $V_w(k)$  and wind direction  $\varphi(k)$  to be  $V_w(k) = 8 + 2 \sin(0.005\pi k + \pi/6) \sin(0.01\pi k)$  [m/s] and  $\varphi(k) = \frac{2\pi}{5} + \frac{\pi}{4} \cos(0.004\pi k)$  [radians].

We mesh the neighborhood of the freeway into a grid of square cells of dimension 200 m as shown in Fig. 2. This means that there are 12 000 m/200m=60 cells along the freeway stretch and 5 cells from the center of the freeway to the center of the target zone. This means that at least  $5 \times 60 = 300$  emission-dispersion states have to be updated every simulation time step. The simulation period is 1 h with a simulation time step of  $T = 10$  s.

As a performance measure of the parametrized MPC controllers, we use the multi-objective function defined in (6). In all these combinations  $\zeta_4 = 0.01$ , because we want to give less emphasis on the variation of the control inputs. We select  $\mu_{CO} = \mu_{HC} = \mu_{NO_x} = 1$ , the  $\mu_{CO_2} = \mu_{FC} = 0$ . The values of  $\zeta_1$ ,  $\zeta_2$ , and  $\zeta_3$  are varied depending on the emphasis we want to induce to the controller performance. In particular we consider four different combinations:  $[\zeta_1 \zeta_2 \zeta_3] \in \{[100], [010], [001], [1011]\}$ . Moreover, we take the prediction horizon  $N_p = 15$  min, the control horizon  $N_c = 10$  min, and the control time step  $T_c = 2$  min. To solve the MPC optimization problem, we use multi-start sequential quadratic programming (SQP) with 8 initial points.

The results of the simulation for the different scenarios are presented in Table I. The first column lists the objective considered in each scenario and the remaining columns list the values of the performance measures (TTS denoting the total time spent, TE denoting the total emissions, and TMDL the total maximum dispersion level at the target zone). Negative percentage values indicate the increment of the performance measures with respect to the uncontrolled scenario (since we want to minimize the performance measures, negative percentages correspond to desired situations), while positive percentages indicate an increment.

When the objective of the controller is set to reduce the

TTS only, the controller reduces the TTS by about 36% while the TE and the TMDL increase by 11% and 30% respectively (see Table I). On the contrary, if the focus of the controller is set to improve the emissions (TE) or the total maximum dispersion level at the target zone (TMDL), the TTS worsens by almost 18% and the TE and TMDL are improved by more than 47% and 51% respectively. The last scenario considers a multi-objective criterion that considers a weighted sum of TTS, TE, and TMDL, which allows to obtain a balanced trade-off between the various control objectives. In this case, the TTS is impacted by about 6% less than in the case where the focus is only on minimizing emissions or the dispersion level at the target zone.

## VI. CONCLUSIONS AND FUTURE WORK

We have proposed a new cell-based emissions dispersion model that is very fast and that is excellently suited for use in on-line model-based traffic control approaches such as MPC. In addition, we have adopted a parametrized MPC approach, in which parameters of feedback control laws are optimized, in contrast to input sequences as is done in conventional MPC. As a result parametrized MPC is much faster than conventional MPC. The resulting MPC approach allows to obtain a balanced multi-criterion trade-off between reduction of travel times, emissions, and fuel consumption. The approach has been illustrated using a simple case study involving variable speed limits and ramp metering.

Future research topics include a more detailed assessment of the new dispersion model, including a comparison with microscopic, more detailed, but much slower dispersion models, the chemistry involved, additional case studies, and extension to other control measures. Moreover, comparison of the proposed approach with existing TMCs and implementation issues of the approach.

## ACKNOWLEDGMENTS

Research supported by the Shell/TU Delft Sustainable Mobility program, the Transport Research Center Delft, the European COST Actions TU0702 and TU1102, the European 7th Framework Network of Excellence "Highly-complex and networked control systems (HYCON2)", and the BSIK project "Next Generation Infrastructures (NGI).

## REFERENCES

- [1] C. M. Benedek and L. R. Rilett, "Equitable traffic assignment with environmental cost function," *Journal of Transportation Engineering*, vol. 124, no. 1, pp. 16–22, Jan.–Feb. 1998.
- [2] S. K. Zegeye, B. De Schutter, J. Hellendoorn, and E. A. Breunese, "Model-based traffic control for the reduction of fuel consumption and emissions, and travel time," in *mobil.TUM 2009 - International Scientific Conference on Mobility and Transport - ITS for larger Cities*, Munich, Germany, May 2009, CD ROM.
- [3] J. B. Rawlings and D. Q. Mayne, *Model Predictive Control: Theory and Design*. Madison, Wisconsin, USA: Nob Hill Publishing, 2009.
- [4] T. Bellemans, B. De Schutter, and B. De Moor, "Model predictive control for ramp metering of motorway traffic: A case study," *Control Engineering Practice*, vol. 14, no. 7, pp. 757–767, Jul. 2006.
- [5] A. Hegyi, B. De Schutter, and H. Hellendoorn, "Optimal coordination of variable speed limits to suppress shock waves," *IEEE Transactions on Intelligent Transportation Systems*, vol. 6, no. 1, pp. 3600–3605, Mar. 2005.

- [6] L. B. de Oliveira and E. Camponogara, "Multi-agent model predictive control of signaling split in urban traffic networks," *Transportation Research Part C*, vol. 18, no. 1, pp. 120–139, Feb. 2010.
- [7] A. Kotsialos, M. Papageorgiou, M. Mangeas, and H. Haj-Salem, "Coordinated and integrated control of motorway networks via non-linear optimal control," *Transportation Research Part C*, vol. 10, no. 1, pp. 65–84, Feb. 2002.
- [8] R. Carlson, I. Papamichail, M. Papageorgiou, and A. Messmer, "Optimal mainstream traffic flow control of large-scale motorway networks," *Transportation Research Part C*, vol. 18, no. 2, pp. 193–212, Apr. 2010.
- [9] I. Papamichail, A. Kotsialos, I. Margonis, and M. Papageorgiou, "Coordinated ramp metering for freeway networks – A model-predictive hierarchical control approach," *Transportation Research Part C*, vol. 18, no. 3, pp. 311–331, Jun. 2010.
- [10] A. Messmer and M. Papageorgiou, "METANET: a macroscopic simulation program for motorway networks," *Traffic Engineering and Control*, vol. 31, no. 9, pp. 466–470, 1990.
- [11] A. Kotsialos, M. Papageorgiou, C. Diakaki, Y. Pavlis, and F. Middelham, "Traffic flow modeling of large-scale motorway networks using the macroscopic modeling tool METANET," *IEEE Transactions on Intelligent Transportation Systems*, vol. 3, no. 4, pp. 282–292, Dec. 2002.
- [12] S. K. Zegeye, B. De Schutter, J. Hellendoorn, and E. A. Breunese, "Model-based traffic control for balanced reduction of fuel consumption, emissions, and travel time," in *Proceedings of the 12<sup>th</sup> IFAC Symposium on Transportation Systems*, Redondo Beach, California, USA, Sep. 2009, pp. 149–154.
- [13] —, "Variable speed limits for area-wide reduction of emissions," in *Proceedings of the 13<sup>th</sup> International IEEE Conference on Intelligent Transportation Systems*, Madeira Island, Portugal, Sep. 2010, pp. 507–512.
- [14] —, "Parametrized MPC to reduce dispersion of road traffic emissions," in *Proceedings of The 2011 American Control Conference*, San Francisco, California, USA, Jun.–Jul. 2011, pp. 4428–4433.
- [15] S. K. Zegeye, B. De Schutter, J. Hellendoorn, and E. A. Breunese, "Nonlinear MPC for the improvement of dispersion of freeway traffic emissions," accepted for the *8th IFAC World Congress*, Milan, Italy, Aug.–Sept. 2011.
- [16] K. Ahn, A. A. Trani, H. Rakha, and M. Van Aerde, "Microscopic fuel consumption and emission models," in *Proceedings of the 78<sup>th</sup> Annual Meeting of the Transportation Research Board*, Washington, DC, USA, Jan. 1999, CD-ROM.
- [17] M. T. Oliver-Hoyo and G. Pinto, "Using the relationship between vehicle fuel consumption and CO<sub>2</sub> emissions to illustrate chemical principles," *Journal of Chemical Education*, vol. 85, no. 2, pp. 218–220, Feb. 2008.
- [18] C. J. Baker, "Outline of a novel method for the prediction of atmospheric pollution dispersal from road vehicles," *Journal of Wind Engineering and Industrial Aerodynamics*, vol. 65, no. 1-3, pp. 395–404, 1996.
- [19] D. I. Robertson and R. D. Bretherton, "Optimizing networks of traffic signals in real time—the SCOOT method," *IEEE Transactions on Vehicular Technology*, vol. 40, no. 1, pp. 11–15, Feb. 1991.
- [20] Peek Traffic, "Utopia/spot technical reference manual," Peek Traffic, Amersfoort, The Netherlands, Tech. Rep., Jan. 2002.
- [21] A. Casavola, D. Famularo, and G. Franze, "A predictive control strategy for norm-bounded LPV discrete-time systems with bounded rates of parameter change," *International Journal of Robust and Nonlinear Control*, vol. 18, no. 7, pp. 714–740, Aug. 2007.
- [22] M. V. Kothare, V. Balakrishnan, and M. Morari, "Robust constrained model predictive control using linear matrix inequalities," *Automatica*, vol. 32, no. 10, pp. 1361–1379, 1996.
- [23] J. Löfberg, "Approximations of closed loop minimax MPC," in *Proceedings of the 42<sup>nd</sup> IEEE Conference on Decision and Control*, Maui, Hawaii, USA, Dec. 2003, pp. 1438–1442.
- [24] R. S. Smith, "Robust model predictive control of constrained linear systems," in *Proceedings of the 2004 American Control Conference*, Boston, Massachusetts, USA, Jun. 2004, pp. 245–250.
- [25] P. M. Pardalos and M. G. C. Resende, *Handbook of Applied Optimization*. Oxford, UK: Oxford University Press, 2002.